

General Disclaimer

One or more of the Following Statements may affect this Document

- This document has been reproduced from the best copy furnished by the organizational source. It is being released in the interest of making available as much information as possible.
- This document may contain data, which exceeds the sheet parameters. It was furnished in this condition by the organizational source and is the best copy available.
- This document may contain tone-on-tone or color graphs, charts and/or pictures, which have been reproduced in black and white.
- This document is paginated as submitted by the original source.
- Portions of this document are not fully legible due to the historical nature of some of the material. However, it is the best reproduction available from the original submission.

NATIONAL AERONAUTICS AND SPACE ADMINISTRATION
LUNAR SAMPLE ANALYSIS PROGRAM

CATION DISTRIBUTION STUDIES IN CLINOPYROXENES, OLIVINES AND FELDSPARS
USING MOSSBAUER SPECTROSCOPY OF ^{57}Fe .¹

Final Technical Progress Report
Period ending January 31, 1971

by

Stefan S. Hafner

Principal Investigator: Stefan S. Hafner

Final Report

Prepared under Contract No. NAS-9-8080

by

THE UNIVERSITY OF CHICAGO
DEPARTMENT OF THE GEOPHYSICAL SCIENCES
CHICAGO, ILLINOIS 60637

for

NATIONAL AERONAUTICS AND SPACE ADMINISTRATION
Manned Spacecraft Center
Lunar Receiving Laboratory
Houston, Texas

N71-21451	(JHRU)	(CODE)	(CATEGORY)
	(ACCESSION NUMBER)	(PAGE)	(NASA CR OR TMX OR AD NUMBER)

16

174941

174941

FACILITY FORM 602

¹ Also submitted to the Second Lunar Science Conference, Houston, January 1971.

ABSTRACT

Magnesium in clinopyroxenes with more than 20 percent wollastonite occurs almost exclusively at the M1 position. In calcium-poor pigeonites from rocks 12018, 12021, and 12053 Mg is significantly more disordered. An olivine from 12018 exhibits 20 percent ordering of iron in one of the M-positions. The Mg,Fe^{2+} distribution in clinopyroxenes and olivines is interpreted in terms of equilibrium distribution temperatures estimated from heating experiments and subsolidus cooling history. Fe^{2+} in feldspars occurs at calcium as well as aluminum positions. No Fe^{3+} has been detected in our mineral separates.

Contents

Introduction

Experimental results

Conclusions

Publication list

References

Figure captions

Tables

INTRODUCTION

The Mössbauer absorption spectra of ^{57}Fe in 15 clinopyroxenes, olivines, and feldspars separated from Apollo 11 and 12 rocks, and a pyroxene and a glass specimen from the Apollo 11 soil have been studied. The aim was to obtain information on the oxidation state of iron and the intracrystalline distribution of iron over the nonequivalent lattice sites. The distribution of $\text{Mg}^{2+}, \text{Fe}^{2+}$ over the sites M1 and M2 in natural pyroxenes is known to be dependent on the cooling history of the rock. Similar relationships between $\text{Mg}^{2+}, \text{Fe}^{2+}, \text{M1}, \text{M2}$ and cooling history appear to exist in olivines. We have made a number of heating experiments with clinopyroxenes and olivines to determine the temperatures of equilibrium distribution in the natural crystals, and to investigate the ordering and disordering kinetics of the $\text{Mg}^{2+}, \text{Fe}^{2+}$ exchange between the M1 and M2 sites.

EXPERIMENTAL AND RESULTS

X-ray emission microanalysis, Mössbauer spectroscopy and heating experiments were carried out as described previously¹. The chemical compositions of the clinopyroxene separates from Apollo 11 and 12 are plotted on to the pyroxene quadrilateral En-Di-Hd-Fs in Figure 1. Plotted along the En-Fs join are the compositions of the olivines from 12053-79 and 12018,35. Site occupancy data for the Apollo 12 clinopyroxenes are given in Table 1. Similar data on the Apollo 11 samples

were reported in reference 1, Table 6.

The Mössbauer spectra of ^{57}Fe in olivines were measured at absorber temperatures between 300 and 500°C since the quadrupole doublets at M1 and M2 are best resolved in that range². Spectra of an iron-rich olivine (Rockport fayalite, Fa_{97}) and an iron-poor sample (rock 12018,35 Fa_{36}) are compared in Figure 2. The resolution of both the high and low velocity doublets shown in this figure is characteristic of the olivine solid solutions. We generally take the area ratio of the high velocity peaks as a measure for the distribution of Fe^{2+} over M1 and M2. Unfortunately the assignment of the doublets to the M-sites is not possible at this time². The results which include distribution data of five terrestrial samples are shown in Table 2.

CONCLUSIONS

Oxidation state of iron

Ferric iron was not detected in any of the separates from the rocks or the soil. In clinopyroxenes the $\text{Fe}^{3+}/(\text{Fe}^{2+} + \text{Fe}^{3+})$ ratio was 0 ± 0.002 ; in the pyroxene and glass separates from soil 10084 this ratio was 0 ± 0.01 . Approximately 7 percent of the total iron in this soil was metallic³. The spectrum is indicative of the presence of some iron in a paramagnetic state (less than 3 percent).

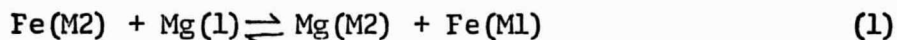
Distribution of iron in feldspars

Iron in the plagioclase feldspars from 10044 and 12021 is in the ferrous state and occurs at two nonequivalent positions with different coordination. The nuclear quadrupole splittings, isomer shifts, line-widths and area ratios are shown in Table 3. Pattern 1 probably results

from Fe^{2+} at the tetrahedrally coordinated Al^{3+} positions whereas pattern 2 may be assigned to the Ca-sites.

Distribution of iron in clinopyroxenes

The exchange energy of the reaction



in pyroxenes within the enstatite-diopside-hedenbergite-ferrosilite quadrilateral is primarily determined by the amount of calcium present at the M2 sites, i.e. the amount of wollastonite component in the solid solution. Space group symmetry and the presence of small amounts of foreign cations at the M-sites appear to be of minor importance. Our limited data suggest a simple, linear relationship between the standard Gibbs-free energy difference, ΔG_E^0 and the wollastonite concentration; but more data will be needed to establish this precisely. Based on this assumption, plots of temperature versus the equilibrium distribution constant k can be drawn where k is equal to the ratio $(\text{Fe}/\text{Mg})_{\text{M1}}/(\text{Fe}/\text{Mg})_{\text{M2}}$. The equilibrium temperature which corresponds to the observed Mg,Fe site occupancy (Table 1) can thus be determined from this plot. This principle is shown in Figure 3.

ΔG_E^0 in clinopyroxenes with Wo_{25-36} is approximately 8-10 kcal per formula unit $\text{M}_2\text{Si}_2\text{O}_6$. Therefore, only very small changes in the equilibrium site occupancy of Mg and Fe at M1 and M2 are expected in the temperature range from 0 to 1000°C. This has been confirmed by experiments (Table 1). Precise occupancy determinations are hampered

by the large chemical zoning and the pigeonite exsolution, characteristic of these crystals. Our data indicate, however, complete ordering, at least within the experimental error, with Mg exclusively at the M1 sites (cf. also ref. 1). We do not believe that there is any indication of Ca disordering. The apparent excess of cations Ca and Fe at M2 in some samples of Table 1 can be largely accounted for by corrections which result from the elements Ti, Mn, Cr, Al.

ΔG_E^0 in apparently homogeneous pigeonites with compositions Wo_{5-10} is approximately 4-5 kcal per formula unit. Disordering as well as ordering experiments of the yellow-green colored pigeonite, 12021,150 suggest a close similarity to that of the orthopyroxene system⁴. Some data for ortho- and clinopyroxenes with compositions within the pyroxene quadrilateral are plotted in Figure 3. The natural Mg,Fe distribution observed in the yellow-green pigeonite 12021,150-P1 corresponds to an equilibrium temperature of 570°C. This temperature is substantially lower than the quench-in temperature for the short range ordering (rate constant K'_{12} , cf. ref. 1) which was determined from an ordering experiment (Table 1) to be 810°C. The natural Mg,Fe distributions in orthopyroxenes from Hawaiian lavas¹ correspond to equilibrium temperatures generally higher than the quench-in temperature for orthopyroxenes. The Mg,Fe distribution observed in the pigeonite 12053,79-P1 (Table 1) represents an equilibrium temperature of 710°C. Ordering experiments have not been carried out but the equilibrium temperature does suggest a more rapid cooling of rock 12053 through the critical range of 600-500°C, compared with rock 12021.

In clinopyroxenes with compositions Wo_{10-20} the observed degree of Mg,Fe disorder over M1 and M2 is high. It seems likely that the ordering processes in these chemically inhomogeneous pyroxenes are hindered by the complexity of the augite-pigeonite exsolution.

Distribution of iron in olivines

The natural Mg,Fe distribution in an olivine separate (Fa_{36}) from rock 12018 exhibits approximately 20 percent more iron in one of the two nonequivalent M-positions (Table 2). After heat treatment at $1155^{\circ}C$ for 7 days the distribution was found to be almost completely disordered. A somewhat ordered terrestrial olivine (B1) did not show disorder after heating at $915^{\circ}C$ for 1 day or $1050^{\circ}C$ for 5 days. It appears that the Mg,Fe exchange in olivines is quenched-in at much higher temperatures than in pyroxenes. But more experiments will be needed on olivines to establish the nature of this exchange reaction between the M-sites and its relationship to the cooling history of the mineral.

Publications

H. Fernandez-Moran, S.S. Hafner, M. Ohtsuki and D. Virgo: Mössbauer effect and high-voltage electron microscopy of pyroxenes in Type B samples. Science, 167, 686-688 (1970).

H. Fernandez-Moran, M. Ohtsuki, S.S. Hafner and D. Virgo: High voltage electron microscopy and electron diffraction of lunar pyroxenes. Proc. Apollo 11 Lunar Sci. Conf. Vol. 1, 409-417 (1970).

S.S. Hafner and D. Virgo: Temperature-dependent cation distributions in lunar and terrestrial pyroxenes. Proc. Apollo 11 Lunar Sci. Conf. Vol. 3, 2183-2198.

S.S. Hafner, B. Janik and D. Virgo: State and location of iron in Apollo 11 samples. Mössbauer Effect Methodology Vol. 6 (E. Gruverman ed.), 193-207 (1971).

Submitted, being submitted: Three additional papers on Apollo 11 and 12 samples.

References

1. S.S. Hafner and D. Virgo: Temperature dependent cation distributions in lunar and terrestrial pyroxenes. Proc. Apollo 11 Lunar Sci. Conf. Vol. 3, 2183-2198 (1970), and references therein.
2. W.R. Bush, S.S. Hafner, and D. Virgo: Some ordering of iron and magnesium at the octahedrally coordinated sites in a magnesium-rich olivine. Nature 227, 1339-1341 (1970).
3. S.S. Hafner, B. Janik, and D. Virgo: State and location of iron in Apollo 11 samples. Mössbauer Effect Methodology Vol. 6, 193-207 (1971).
4. D. Virgo and S.S. Hafner: Fe^{2+} , Mg order-disorder in heated orthopyroxenes. Mineral. Soc. Amer. Spec. Pap. 2, 67-81 (1969), and references therein.

Figure captions

- Fig. 1. Average compositions (molecular percents) of clinopyroxene separates from rocks 12018 (\square), 12021 (\times) and 12053 (Δ). The compositions of two olivine separates from 12018 (\boxplus) and 12053 (Δ) are plotted on the En-Fs join. Also plotted are the previously published data from Apollo 11 rocks¹.
- Fig. 2. ^{57}Fe resonant absorption spectra of an olivine separate from rock 12018 Fa_{36} (top), and a fayalite Fa_{97} (bottom).
- Fig. 3. Plot of temperature against the equilibrium distribution constant $k = (\text{Fe}/\text{Mg})_{\text{M1}}/(\text{Fe}/\text{Mg})_{\text{M2}}$ for orthopyroxenes $((\text{Mg},\text{Fe})\text{SiO}_3)$; pigeonite 12021, 150-P1 $((\text{Mg},\text{Fe})_{0.93}\text{Ca}_{0.07}\text{SiO}_3)$; pigeonite 12053, 79-P1 $((\text{Mg},\text{Fe})_{0.90}\text{Ca}_{0.10}\text{SiO}_3)$, and augite 10044, 26-P2 $((\text{Mg},\text{Fe})_{0.64}\text{Ca}_{0.36}\text{SiO}_3)$. The slopes of the lines are constructed assuming a constant standard Gibbs free energy, ΔG_E^0 , determined from a linear plot of ΔG_E^0 and molecular percent

Fig. 3. wollastonite in the sample (numbers in kcal per mole). The (cont'd.) crosses (X) correspond to the respective measured k values for the unheated samples. For the orthopyroxene line, the crosses correspond to volcanic samples from Hawaii¹. The circles (O) correspond to the final distributions in ordering runs of initially disordered samples. For the $(\text{Mg,Fe})_{0.93}\text{Ca}_{0.07}\text{SiO}_3$ and $(\text{Mg,Fe})\text{SiO}_3$ samples, these were respectively 600°C for 7 days and 550°C for 7 days.

Table 1 Estimated Mg, Fe, Ca site occupancies in clinopyroxenes from Apollo 12.

Clinopyroxene	En	Fs	Wo	$\frac{A(Ml)}{A(tot)}$	$\frac{I(Ml)}{I(tot)}$	Estimated site occupancy			
						Mg	$\frac{Ml}{Fe}$	Ca	$\frac{M2}{Fe}$
12018, 35-P1	50	35	14	0.250	0.263	0.814	0.186	-	0.192 0.520 0.288
12018, 35-P2	46	41	13	0.332	0.351	0.715	0.285	-	0.212 0.527 0.261
12021, 150-P1 natural	61	33	6	0.176	0.189	0.873	0.127	-	0.343 0.543 0.114
12021, 150-P1 555°C	61	33	6	0.172	0.186	0.875	0.125	-	0.341 0.545 0.114
12021, 150-P1 800°C	61	33	6	0.248	0.258	0.827	0.173	-	0.389 0.497 0.114
12021, 150-P1 1000°C	61	33	6	0.273	0.290	0.806	0.194	-	0.410 0.476 0.114
12021, 150-P1 1000°C, 600°C	61	33	6	0.234	0.253	0.831	0.169	-	0.386 0.500 0.114
12021, 150-P2	31	42	27	0.401	0.403	0.618	0.342	-	- (0.506) (0.533)
12021, 150-F2 800°C	31	42	27	0.418	0.430	0.618	0.365	-	- (0.483) (0.533)
12021, 150-P2 1000°C	31	42	27	0.414	0.448	0.618	0.380	-	- (0.468) (0.533)
12021, 150-P3	17	56	27	0.506	0.516	0.335	0.581	-	- (0.545) (0.539)
12053, 79-P1	59	31	10	0.183	0.220	0.861	0.139	-	0.314 0.492 0.194

Table 2. Nuclear hyperfine doublets of ^{57}Fe in olivines: line widths and area ratios.

Olivine	Composition mol. percent Fa	Absorber temperature $^{\circ}\text{C}$	Line widths (FWHH) (mm/sec)			Area ratios ^a	
			A_1^a	A_2^a	B_1	$\frac{B_1 + B_2}{\text{total area}}$	$\frac{B_1}{B_1 + B_2} = \frac{\text{Fe}_1^{2+}}{\text{Fe}_1^{2+} + \text{Fe}_2^{2+}}$
<u>Apollo 12</u> 12018, 35-01 (natural) " " 12018, 35-01 (1155 $^{\circ}\text{C}$, 7 days) " " " " " "	36	273	0.300	0.312	0.241	0.507	0.422
	36	315	0.305	0.297	0.222	0.497	0.416
	36	350	0.306	0.285	0.207	0.491	0.394
	36	303	0.326	0.299	0.265	0.492	0.464
	36	316	0.304	0.273	0.229	0.490	0.448
	36	353	0.306	0.263	0.239	0.488	0.467
	36	402	0.331	0.275	0.278	0.488	0.506
	97	269	0.222	0.257	0.221	0.493	0.500
	97	336	0.227	0.241	0.224	0.495	0.506
	97	368	0.227	0.243	0.219	0.494	0.508
	97	420	0.224	0.243	0.219	0.494	0.500
	74	315	0.364	0.297	0.286	0.485	0.489
<u>Terrestrial</u> Rockport fayalite " " " " " " Ho-A " " B-16 " " " " Modoc " "	74	571	0.361	0.291	0.302	0.485	0.485
	23	273	0.330	0.361	0.275	0.509	0.381
	23	334	0.333	0.323	0.288	0.502	0.454
	23	372	0.340	0.335	0.281	0.501	0.429
	22	353	0.335	0.307	0.298	0.497	0.501
	22	431	0.330	0.302	0.286	0.496	0.497

Table 2. (continued)

Olivine	Composition mol. percent Fa	Absorber temperature °C	Line widths (FWHH) (nm/sec)			Area ratios ^a	
			A ₁ ^a	A ₂ ^a	B ₁	$\frac{B_1 + B_2}{\text{total area}}$	$\frac{B_1}{B_1 + B_2} = \frac{Fe_1^{2+}}{Fe_1^{2+} + Fe_2^{2+}}$
Bl (natural)	18 18	301 337	0.280 0.284	0.274 0.274	0.227 0.232	0.494 0.495	0.451 0.452
Bl (915°C 1 day)	18	360	0.326	0.309	0.282	0.498	0.445
"	18	390	0.322	0.298	0.273	0.492	0.456
"	18	510	0.332	0.311	0.294	0.494	0.470
Bl (1055°C, 5 days)	18	341	0.297	0.282	0.245	0.498	0.450
"	18	376	0.302	0.287	0.252	0.498	0.449
"	18	412	0.301	0.282	0.250	0.497	0.452
Sl4	8	416	0.315	0.297	0.286	0.495	0.486
"	8	460	0.314	0.305	0.287	0.497	0.486

^a Determined from four-line fits (13 variables) in the case of fayalite and from three-line fits (10 variables) for the remaining samples; A and B refer to the low and high velocity peaks of the doublets, respectively (cf. Fig. 2).

Table 3. Hyperfine interaction of ^{57}Fe in lunar feldspars at 298^oK.

Specimen	Wt. percent natural iron	Quadrupole splitting		Isomer shift ^b	
		1 mm/sec	2 mm/sec	1 mm/sec	2 mm/sec
10044,26	0.4 ^a	1.54	2.01	0.90	1.13
12021,150	?	1.49	2.03	0.87	1.13
	Peak widths			Area ratio (2)/(1+2)	
	<u>A</u> mm/sec	<u>B</u> mm/sec	<u>C</u> mm/sec		
1044,26	0.52	0.35	0.65	0.65	
12021,150	0.51	0.36	0.65	0.88	

^afrom J. V. Smith et al., Proc. Apollo 11 Lunar Sci. Conf. Vol. 1, 897-925 (1970)

^breferred to a metallic iron absorber

Fig. 2

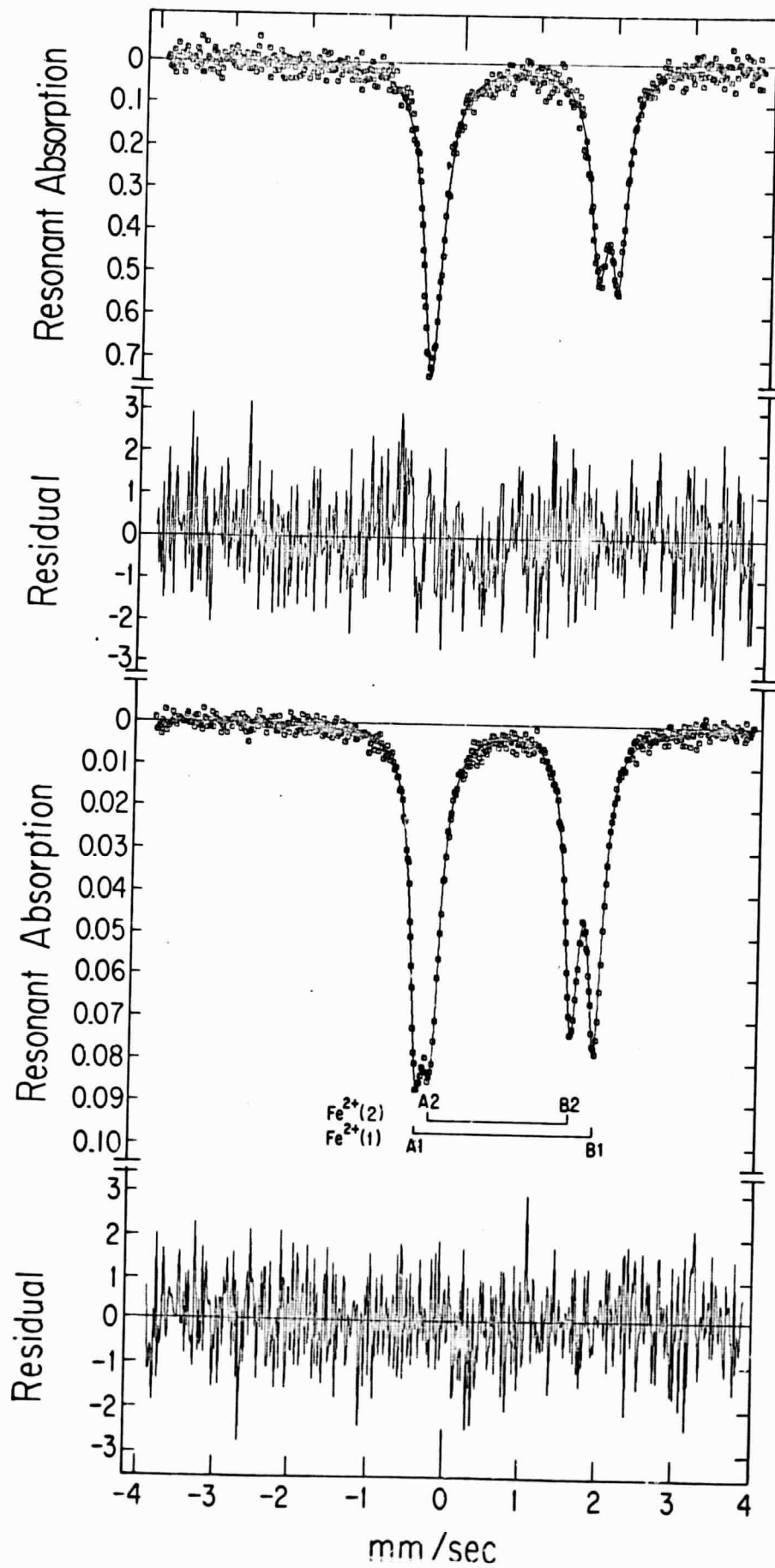


Fig. 3

